


Yielding and Flow in Aggregated Particulate Suspensions

Peter J. Scales¹  · Shane P. Usher¹ ·
Maria Barmar Larsen² · Anthony D. Stickland¹ ·
Hui-En Teo¹ · Ross G. de Kretser¹ · Richard Buscall³

Received: 14 November 2022 / Accepted: 25 July 2023
© Crown 2023

Abstract The flow and consolidation of strongly flocculated particulate suspensions in water are common to a range of processing scenarios in the minerals, food, water and wastewater industries. Understanding the compressive strength or resistance to consolidation of these suspensions is relevant to processes such as filtration, centrifugation and gravity settling, where the compressive strength defines an upper boundary for processing. New data for the compressive strength of consolidating flocculated particulate suspensions in water, including alumina and calcium carbonate, are compared with earlier data from the literature and from our own laboratories for several systems, including two earlier sets of data for alumina. The three sets of data for the compressive strength of alumina agree well. Differences are noted for data measured in shear between our own laboratories and others. New data for the shear strength of AKP-30 alumina are also presented, and although the agreement is not as good, the difference is implied to be due to wall slip associated with a difference in measurement techniques. A simple nonlinear poro-elastic model of the compressive strength was applied to the eight sets of compressive strength data and was found to account for most features of the observed behaviour. The agreement strongly supports the mechanistic failure mode in compression for these systems to be one of simple strain hardening. The one feature that it does not account for without invoking a ‘ratchet’ is

the irreversibility of consolidation. It is, however, suspected that wall adhesion might provide such a ratchet in reality, since wall adhesion has been neglected in the analysis of raw compressive strength until recently, notwithstanding the pioneering work of Michaels and Bolger (30). Overall, the data analysis and fitting presented herein indicate a new future for the characterisation of aggregated particulate suspensions in shear and compression whereby a limited data set in both compression and shear, albeit targeted across a wide concentration range, can now be used to predict comprehensive curves for the shear yield stress and compressive yield stress of samples using a simple poro-elastic model. The veracity of the approach is indicated through a knowledge that the behaviour of both parameters is scalar across a wide range of materials and across a wide range of states of aggregation.

Keywords Shear yield stress · Compressive yield stress · Suspension aggregation · Mode of failure

1 Introduction

Strongly flocculated particulate suspensions in water are typical of industries from mining to wastewater processing. Above a critical solids concentration (denoted as the gel point, ϕ_g), these suspensions show an activation barrier to the initiation of flow (yielding behaviour) in both shear and compression. At increasing solids concentrations, the force to initiate flow behaviour rises in an exponential fashion [1]. The measurement of yielding in shear (σ_y) was simplified by Nguyen and Boger [2, 3] with the introduction of the vane shear yield stress method, although a range of authors had previously reported apparent or Bingham yield stress values in flocculated suspensions through extrapolation of shear stress–shear rate rheological data to zero shear rate.

✉ Peter J. Scales
peterjs@unimelb.edu.au

¹ Centre of Excellence for Enabling Eco-Beneficiation of Minerals, Department of Chemical Engineering, University of Melbourne, Melbourne, VIC 3010, Australia

² Department of Chemistry and Bioscience, University of Aalborg, Aalborg, Denmark

³ Maritime Court, Exeter EX2 8GP, UK

The latter are not considered here since the study of yielding is, at a philosophical level at least, a static to dynamic transition rather than the opposite.

Measurement of a peak stress in shear during constant rate flow start-up has been taken across a wide range of particulate suspensions with systematic changes noted as a function of solid concentration and other parameters that are known to change the strength of interparticle attraction, for example, pH, salt concentration or the addition of simple molecular additives [1, 4–9]. Phenomenological modelling of these same systems demonstrated that the changes in shear yield stress as a function of parameters such as pH, salt concentration and even ion type [10, 11] are scalar as a function of solids concentration. This indicates that the mechanism of failure (yielding) and initiation of unsteady flow in these systems is cooperative. Some authors hypothesised that this scalar correlation to the strength of adhesion between particles implied that the measured shear yield stress was a pseudo-material property, although such an analogy was treated with a useful level of scepticism [12]. None the less, most researchers and practitioners in particulate processing were happy to accept that its measurement was useful for a range of process control scenarios relating to flow, mixing and pipeline start-up, with empirical measurements common [13].

More recent research of the mechanism of yielding in shear has shown that the process can be described well by an analogy to cage melting [14] whereby under an applied stress, the particulate network first strain hardens followed by interparticle bond breakage. At low solids concentrations, the system then yields and flows, with the strain at the point of yield consistent with the interparticle interaction length. However, the more usual observation for systems with a concentration much greater than ϕ_g is that after bond breakage, the network undergoes Brownian reformation that is in competition with the rate of shear, and hence, we observe shear dependent strain softening leading to cage melting (yielding) [15–17]. At higher strains, we then see unsteady–steady flow. The strain at yield is typically of order 1, consistent with the cage melting analogy, and the measured yield stress is dependent on the rate of measurement. Aiding the previous debate [12], the more detailed analysis demonstrates that the measured shear yield stress is not a singular parameter for flocculated suspensions. Indeed, Nguyen and Boger [2] demonstrated this behaviour in their early work and chose a rotation rate for their vane shear yield stress measurements based on the minimum in the observed peak stress.

Systematic data for yielding in compression are not as widely reported although work by Channell and Zukoski [18], Green et al. [19] and the extensive work by Zhou et al. [20, 21] indicates a systematic scalar relationship between the peak stress measured in shear (σ_y) and the pressure required to achieve the same solids concentration at

equilibrium through uniaxial compression. The latter data have been typically achieved through filtration tests to equilibrium although data closer to the gel point are sometimes measured through either sedimentation [22, 23] or centrifugal methods [24].

As indicated, these flocculated (strongly cohesive) particulate suspensions undergo differential compression when they consolidate under gravity, or in a centrifuge, or when they are pressure-filtered or dried, whereby the particulate network reduces in volume as liquid is expelled. This is consistent with the original concept of poro-elastic materials whereby the deformation of the porous (usually water-filled) space between the particles causes fluid displacement. In highly elastic systems, it would be expected that deformation and reformation might be synonymous although this is not expected to be the case in weakly elastic cohesive suspensions at large strain. Since the particles are sticky and a finite volumetric strain cannot sensibly be distinguished from a change in volume fraction, the volumetric Hencky strain (ϵ_H) is taken to be given by [25]:

$$\delta\epsilon_H = \delta\ln\phi \quad (1)$$

and the bulk modulus by:

$$K(\phi) = dP(\phi)/d\ln\phi \quad (2)$$

A simple prescription for the compressive strength (P) then follows; thus,

$$P(\phi) = \int_{\phi_0}^{\phi} K(x)d\ln(x) = a \int_{\phi_0}^{\phi} G(x)d\ln(x) \quad (3)$$

where G is the shear modulus and the order-one constant a is equal to 5/3 for the case of central forces only (by way of illustration). It follows from Eq. 3 that, strictly, $P = P(\phi, \phi_0)$, although the dependence on the starting concentration (ϕ_0) is predicted to be weak when the modulus increases rapidly with concentration, as it does in practice (typically $\phi^{4.5 \pm 0.5}$) [18, 21, 25–27]. Hence, it is usually found that $P \approx P(\phi)$, i.e. the compressive strength looks like a pseudo-material property, also referred to as the compressive yield stress.

It is usually found also that compression is largely irreversible (there is sometimes some minor recovery), which is at odds with the above poro-elastic prescription, from which one would expect 20% or more recoverable strain, depending upon volume fraction, given the exponent of ~ 4 . The particles are, however, adhesive and stick to the walls of the vessel, so a ‘ratchet’ [28, 29] can be invoked to explain this feature. It has been found also that above the gel point a critical level of pressure needs to be exceeded before anything happens [25]; this being why $P(\phi)$ is often called the compressional yield stress. This feature certainly is at odds with the above relationship. There is, however, a reluctance

to abandon Eq. 3 nevertheless, because it does account for one very significant and widespread finding, viz. that $P \sim K \sim G > \sigma_y$ (away from the gel point). Flocculated particulate suspensions are, however, usually adhesive as well as cohesive and wall adhesion can explain this anomaly on laboratory scales, since yield at the walls is a necessary precursor to compression [30, 31].

The adhesion can be characterised by a wall shear stress σ_w [30], related to the bulk yield stress by,

$$\sigma_w \leq \sigma_y \equiv \gamma_c G, \quad (4)$$

where γ_c is the apparent yield strain, defined as the ratio of yield stress to linear modulus. This definition adds nothing as such, but it provides a very convenient way of parameterising adhesive strength [31, 32].

Wall adhesive effects are expected to be unimportant when [30, 32]:

$$\frac{20L\gamma_c G(\phi)}{3wP(\phi)} \ll 1, \quad (5)$$

where w and L are the horizontal width and vertical length of the sample, but significant otherwise. It is also easy to show from Eqs. 3 and 4 that wall effects are *always* expected to be important when and where the volume fraction is very close to either the starting concentration, ϕ_0 , or the gel point ϕ_g , whichever is the greater, almost regardless of the value of γ_c .

2 Experimental Section

This work looks at historical published data as well as some new laboratory data. The historical data were taken from various publications and include work on attapulgitic clay, silica and latex (Buscall et al., [33]), alumina (Channell and Zukoski [18], Zhou et al. [21]) and kaolin (Aziz et al. [34]). The new data were generated with two types of materials, namely AKP-30 alumina (labelled Kristjansson herein) and calcium carbonate (labelled HE Teo herein). The alumina was an aluminium oxide (99.99%, AKP-30, Sumitomo Shoji Chemicals Co., Tokyo, Japan). The 360 nm alumina particles were suspended in a 10^{-2} M KNO_3 solution and sonicated at 200 Watt (Branson Sonifier 450) for 2 min to break up lumps, with the pH adjusted to 5. After further sonication for 1 min, the suspension was then allowed to rest for 24 h. The calcium carbonate was an industrial sample from Omya, Australia (Omyacarb 2) and was dispersed as for the alumina with a sonication horn but at pH 11. Prior to measurement, the suspension was coagulated at its isoelectric point (pH 8.0 ± 0.1) and allowed to equilibrate for 2 h. The Sauter mean diameter of the calcium carbonate was $4.5 \mu\text{m}$ (Malvern Mastersizer 2000).

The AKP-30 alumina was aggregated in two ways. The first involved coagulation to the isoelectric point of the suspension. In this case, the pH of the suspension was adjusted to 9.0 ± 0.1 and allowed to rest for two hours prior to measurement. Different volume fractions were obtained by diluting a stock suspension with 0.01 M KNO_3 solution and adjusting the pH. The volume fraction was determined by weight loss on drying, where the samples were left to dry for 24 h at 100°C (Lab-line Due-Vac oven, Melrose Park, ILL).

In the second method of aggregation, suspensions were flocculated with polyacrylic acid and a polyacrylamide polymer. Alumina suspensions with an electrolyte concentration of 10^{-3} M KNO_3 were prepared as described previously. A stock particulate suspension was diluted to 2.5 w/w% with 10^{-3} M KNO_3 solution. The diluted suspensions were then sonicated for 1–2 min and the pH adjusted to 7.29 ± 0.1 . A polyacrylic acid solution (MW = 250,000 g/mol, Aldrich Chemical Company, USA) was prepared at 0.1 w/w% in demineralised water. The solution was stirred for 1 h, to ensure complete dissolution of the polymer, using a magnetic stirrer. A non-ionic polyacrylamide solution (0.2 w/w% Magnafloc LT20) was produced by dissolving the dry polymer in ethanol and mixing it with demineralised water (0.2 g powder to 2 mL ethanol in a 100 mL solution). The covered mixture (to avoid UV degradation of the polymer) was shaken overnight. An hour before flocculation, a 0.01 w/w% solution was produced by diluting and stirring for 1 h.

The suspensions were flocculated in a 1000-ml baffle reactor as described by Holland and Chapman [35]. After 5 min mixing at 500 rpm (Heidolph, RZR 2020 control), the speed was reduced to 330 rpm and the PAA solution was added and mixed for 1 min. After the addition of PAA, the Magnafloc LT20 solution was added to the suspension and mixed for 20 s. The suspension was left for the flocs to settle, and the settling rate was measured. After the flocs had settled, the stirrer and the baffles were removed from the suspension and the supernatant was decanted.

The shear yield stress was measured with a vane on a Haake Viscometer (HAAKE VT550, Karlsruhe, Germany).

Table 1 Vane dimensions employed in shear yield stress measurements

Vane	Height H (mm)	Diameter D_v (mm)
1	15.145	9.96
2	20.20	20.21
3	30.17	25.02
4	50.0	25.0
5	75.0	25.0
6	100	50
7	200	100

A range of vanes were utilised to cover a wide range of peak stresses. The different vane dimensions employed are shown in Table 1. The yield stress measurement was taken by loading the sample in a suitable container and for the sample coagulated to the isoelectric point and then shearing it well to avoid potential thixotropic effects that would influence the results. The vane was lowered into the suspension until the suspension covered the vane, plus a further distance corresponding to the vane radius. The sample was allowed to rest for 2 min. For the polymer-flocculated sample, the suspension was not mixed after loading. A shear rotation rate of 0.2 rpm was then applied to the vane, and the yield stress was calculated according to the method of Nguyen and Boger [2]. The Haake had a limiting torque of approximately 30,000 μNm corresponding to a maximum limiting stress of approximately 10 kPa (using the smallest vane). Data were truncated below 1 Pa as measurement errors, even for the largest vane, became significant below this value.

Compressive yield stress measurements were completed using a combination of sedimentation, filtration [36, 37] and centrifugation tests [38]. Filtration tests were conducted on a piston-driven filtration rig that used a linear encoder to monitor piston height. The device and its operation are described elsewhere [36], inclusive of the measurement of the final volume fraction of suspensions for a given equilibrium filtration pressure. This value was compared to the final volume fraction as determined by weight loss on drying, and the agreement was found to be good.

For centrifugation, the method used polycarbonate centrifuge tubes (Naglene) with a height of 103 mm and inside diameter of 26.5 mm. A flat base inside the tube was formed by adding a small amount of epoxy resin into each tube. The measurement was then taken by measuring the initial

height of the tubes. As the epoxy resin was not completely even, the height was determined with a steel ruler (precision 0.1 mm, digital calliper) from an average value of six measurements round the tube. Sample heights between 7 and 50 mm were employed. The suspensions were tested at 20 °C. The samples were run until equilibrium was obtained (i.e. a constant bed height). The sample was divided into about 10 slices. Each sub-sample was removed by scraping the sample from the tube using a flat spatula fixed at the desired sample height, and the volume fraction for the sub-sample was found by weight loss on drying. Compressive yield stress data were calculated according to the method described by Green and Boger [39].

In sedimentation tests, an initial concentration below the gel point was chosen. Glass measuring cylinders with different initial suspension heights were left to settle and the sediment–liquid interface measured until equilibrium was reached. The final height was then measured and the resulting volume fraction and the compressive yield stress calculated using the final average volume fraction and compressive stress as described in [40]. Compression data were truncated below 100 Pa due to measurement error becoming significant.

3 Results and Discussion

Figure 1a shows a compilation of compressive strength data for some coagulated systems, including extensive data for colloidal alumina from 2 different laboratories and 4 different workers. Most of the suspensions depicted in Fig. 1 comprise either spheroidal or tuberoïdal particles. The particle size range covered is enormous (from 4.5 μm CaCO_3 down

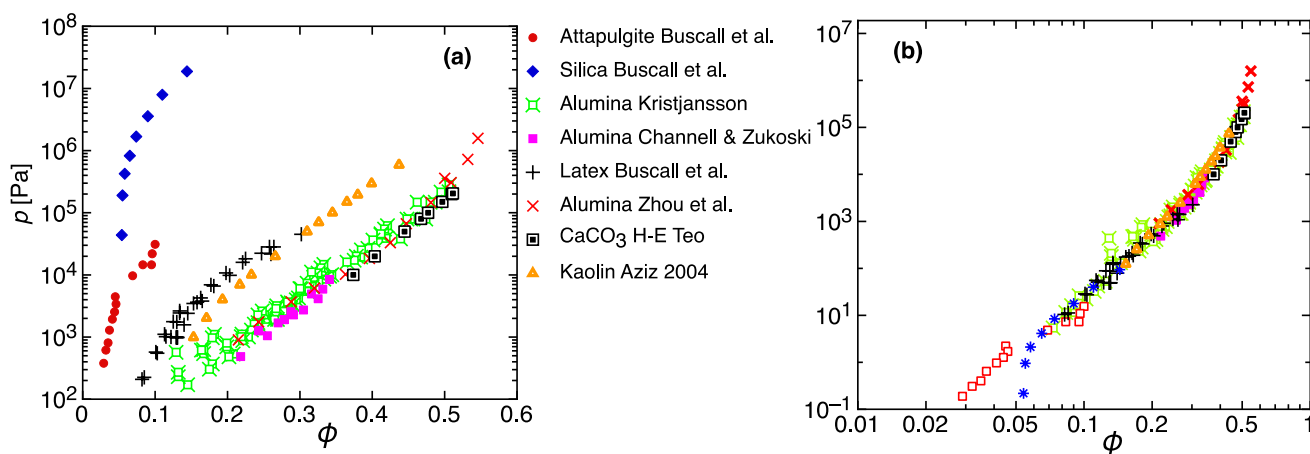


Fig. 1 Plots, semi-log and log, of compressive strength versus volume fraction for a range of inorganic particulate suspensions together with polystyrene latex. The new (unpublished) data for AKP-30 alumina and calcium carbonate are those labelled ‘Alumina Kristjans-

son’ and ‘ CaCO_3 HE Teo’. In **b**, the data in **a** have been scaled by shifting data on the ordinate such that all data go through a fixed point of 20 Pa at a volume fraction of 0.1 (color figure online)

to 26 nm SiO₂), although data for fine kaolin (lozenges) and attapulgite (long needles) are also shown. The data are scaled on the ordinate in Fig. 1b whereby the data have been shifted vertically such that all data match a strength of 20 Pa at a volume fraction of 0.1. Despite an arbitrary reference point in terms of the shift, a master curve results, implying the mechanism of failure to be both consistent and cooperative across a wide range of aggregated colloidal particulates. The only significant departure from the master curve is for SiO₂, which shows an obvious gel point. The SiO₂ gels were, however, very strong by virtue of their small particle size (26 nm diameter) and it was only with this material that the methods used (centrifugation or pressure filtration) could measure near the gel point. The gel point of the colloidal alumina could well be similar to that of the silica though, as it looks to be 0.05 or less; see also Fig. 2, which shows shear yield stress data for the colloidal alumina (this work).

The concentration dependence of the shear yield stress is weaker than that of the compressive yield strength in the power-law region. The power law of 3.0 is typical for shear, whereas the shear storage modulus is found to show a power of > 4 [18, 21, 25, 27]. This tells us that the apparent critical strain defined by the right-hand side of Eq. 4 decreases with concentration.

The shear yield stress data were fitted with the functional form:

$$\sigma_y = k\phi^{3.0}(0.64 - \phi)^{-1.8} \tag{6}$$

with $k = 2400$ Pa (dashed line in Fig. 2).

And the compressive yield stress was fitted with the functional form:

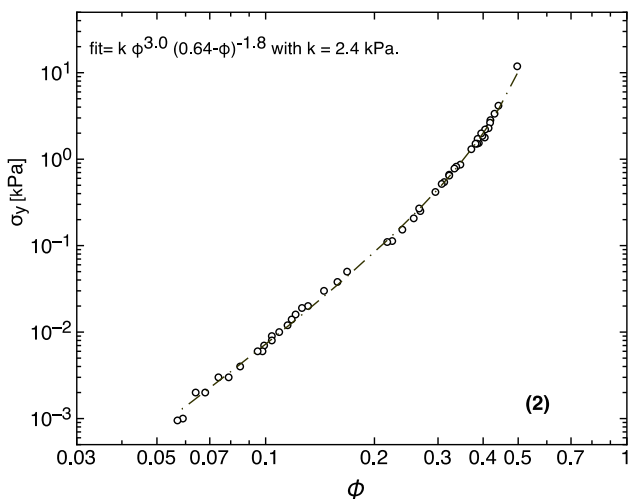


Fig. 2 Plot of shear yield stress data (this work) versus volume fraction for AKP-30 alumina, fitted as shown

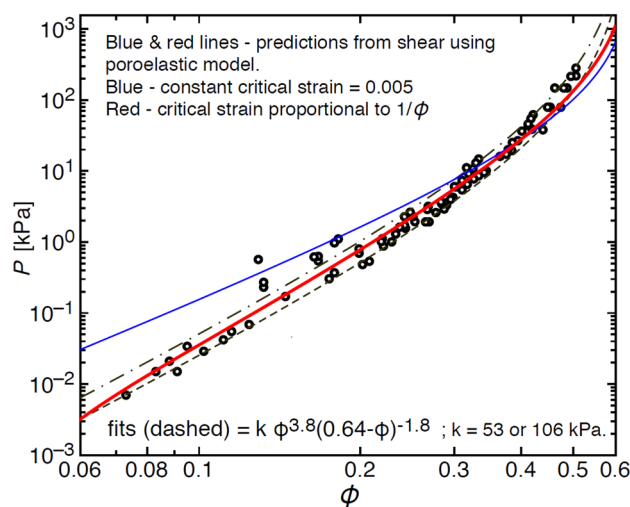


Fig. 3 Compressional stress for AKP-30 alumina, fitted as shown and compared with predictions made from the data in Fig. 2 using Eqs. 3 and 4 (see text)

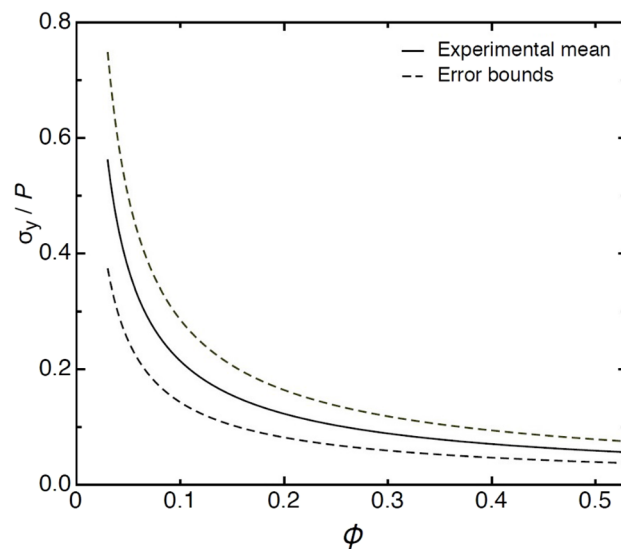


Fig. 4 Plot of shear-to-compressional-strength ratio obtained from the fits shown in Figs. 2 and 3

$$\sigma_y = k\phi^{3.8}(0.64 - \phi)^{-1.8} \tag{7}$$

with $k = 5300$ or $106,000$ Pa (dashed lines in Fig. 4).

If Eq. 3 is correct then, it should be possible to predict the compressive strength from the shear strength using Eqs. (3) and (4). The blue and red lines in Fig. 3 show the results. The blue line has been obtained by supposing that the apparent critical shear strain is constant (and 0.005), which we know it is not, and the red line by assuming that it is proportional to $1/\phi$. The actual fit data are shown in Fig. 3.

The agreement between the red line experimental data is excellent for $\phi < 0.4$. Above 0.4, it is not, although there are good reasons why there might be a difference there, which space does not permit discussing here, except to say that neglect of the osmotic pressure of the particles and the potential for the failure to be dominated by sliding friction at higher solids concentrations are two aspects [41]. The agreement below $\phi < 0.4$ is, however, most gratifying.

Direct experimental evidence in favour of the model encoded in Eqs. 3 and 4 is shown in Fig. 4, where the experimental ratio of shear to compressive strength is plotted against ϕ , together with the experimental uncertainty. The curves imply that the ratio starts at unity and decays rapidly with increasing volume fraction. This is exactly what Eqs. 3 and 4 predict and must happen by embodying the idea that particulate gels are strain-hardening in compression and in shear, showing strain hardening with failure at strains equivalent to the length scale of the interparticle force at low volume fractions but shift to a cage melting behaviour dominated by strain softening in shear as the volume fraction increases. It alone is powerful evidence that Eqs. 3 and 4, simple though they are, capture most of the observed behaviour and that failure in compression is mechanistically simpler than failure in shear, at least at volume fractions away from the gel point. It should be noted though that the compressional data for alumina have not been corrected for wall adhesion, which must contaminate them to some extent at the lowest concentrations [32], doing so, however, can only make the rise towards unity at low concentration in Fig. 4 even steeper, reinforcing the point.

Whereas Fig. 4 contains direct evidence in support of the simple constitutive model embodied in Eqs. 3 and 4, it might be thought that the comparison with predictions made using these equations amounts to little more than curve fitting. This would certainly be true were the choice of the form of the apparent critical strain function to be unconstrained and allowed to float. The argument then lies in having independent evidence in favour of a roughly hyperbolic decrease in the apparent critical strain with volume fraction. That argument is as follows: that it has been widely observed [21, 25, 27, 42] that the exponents of the concentration dependence of the shear yield stress are typically found to be ~ 3 and the shear modulus typically ~ 4 , i.e. they differ by ca. one. The weakness of this argument is that, although we see an exponent of 3 for the yield stress, we do not have a similar comprehensive set of data for the modulus of the alumina itself. Furthermore, we have ignored the shear data of Channell and Zukoski [18] who unusually see the same exponent of ~ 5 for both properties. Not only is the exponent for the shear yield stress very different from ours, the magnitudes are overall dissimilar too, even though the compressive data agree. Their shear data, compared with ours, are shown in Fig. 5.

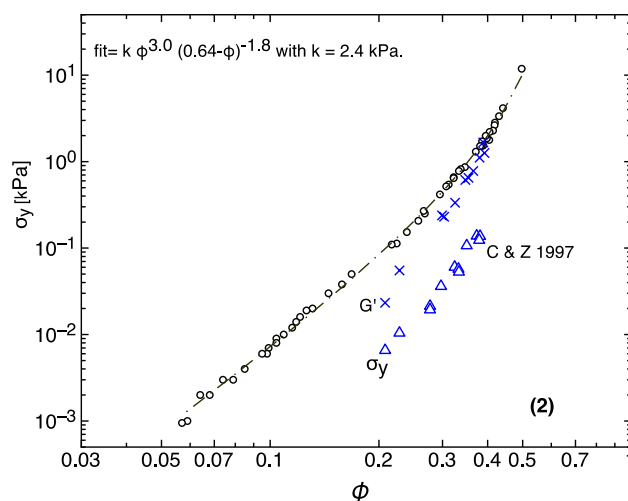


Fig. 5 Comparison of the shear yield stress data (this work) with that of Channell and Zukoski [18]. Their G' (storage modulus) data are also shown

It can be seen that not only are yield stresses in the work of Channell and Zukoski about an order of magnitude smaller on the average, even their shear modulus is smaller than our yield stress. The high exponent and low magnitudes are causes for concern. Unlike us though, Channell and Zukoski used smooth concentric cylinders with small gaps to perform their measurements; hence, a likely explanation of the difference is that they were seeing premature wall yielding and slip [43]. Another possibility is that their material might possibly have undergone the type of shear-induced densification or granulation described by Firth [44] and Mills et al. [42], who showed that shear flow may or may not cause irreversible changes in microstructure, depending upon the detailed nature of the shear rate history. Having said that, the samples herein are stirred prior to measurement and this is an unlikely explanation. We suspect that slip probably suffices to explain the difference, not least because it is known that materials of this type will slip at the outer cylinder, even with vane rotors, should the gap not be wide enough to prevent it [43]. It behoves us then, to repeat the measurements of yield stress and G' using both types of rheometer tool on the same batch of alumina in order to prove the point.

Was the material of construction of our centrifuge tubes were the same as that of Channell and Zukoski's [18] rheometer tools, then we would perhaps have used their shear data, or an extrapolation of it to lower volume fractions, to correct Figs. 4 and 3 for wall adhesion using the methods described by Lester and Buscall [32, 38]. We would, however, have found the error to be insignificant. Until such time as shear data for glass and polycarbonate become available, all that we can do in the first instance is to calculate an upper bound correction from the true or cohesive yield stress. This

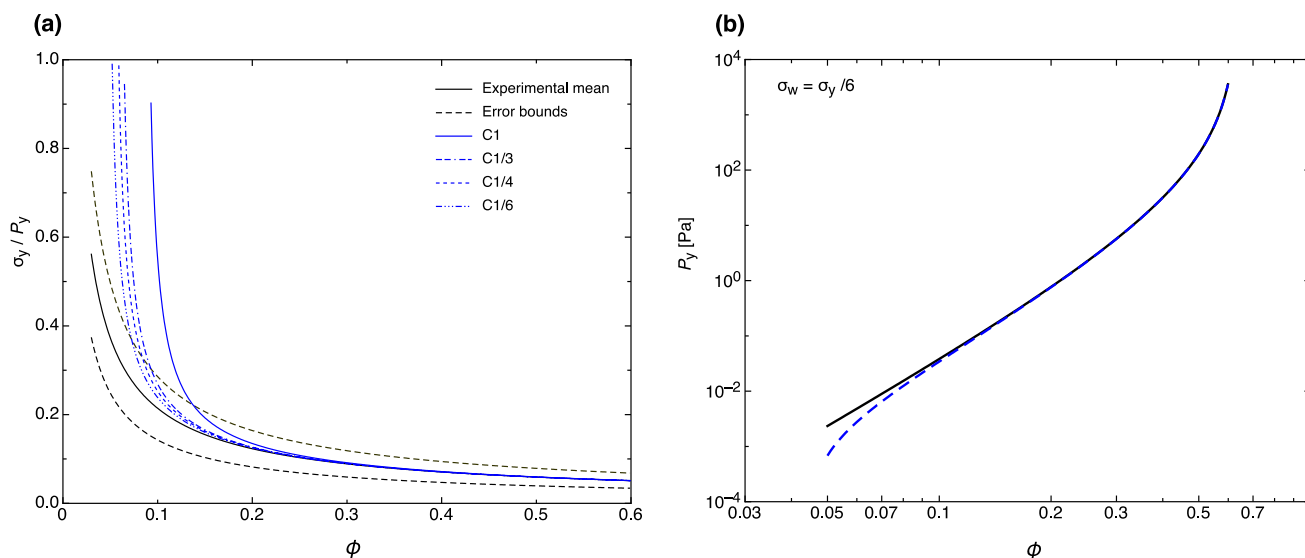


Fig. 6 **a** Over-corrected strength ratios are shown in blue (see text for details) and **b** compressive strength data from Fig. 3 corrected using $\lambda = \sigma_w / \sigma_y = 1/6$ where the solid line is the original data and the dashed line is corrected for wall adhesion

correction (λ) is shown by the continuous blue line labelled C1 in Fig. 6a. C1 assumes that $\sigma_w = \sigma_y$ (i.e. $\lambda = 1$).

We know that C1 is an over-correction because the divergence of the corrected ratio then implies a gel point of ca. 0.09, whereas the σ_y data in Fig. 2 extend below that; they imply a gel point of 0.05 or less perhaps. Thus, what one can then do is to write $\sigma_w = \lambda \sigma_y$, and then find the value of λ by shooting that brings the divergence down to 0.05. In this case, a value of just less than 1/6 is needed in order to cause the strength ratio to diverge at 0.05. The second plot shows the original compressive strength data corrected using $\lambda = 1/6$. The correction is not that large because fairly wide centrifuge tubes (26.5 mm) were used in this case. Such corrections become much more serious at, say, 10 mm or less. It does, however, highlight that the use of narrow centrifuge tubes could lead to the incorrect conclusion that there is no gel point in the system or that the gel point is lower than reality. The implication of the work is that little or no correction would be necessary if wide centrifuge or sedimentation tubes were always utilised (i.e. width of tube of sedimentation column is an order of magnitude larger than the height of the sediment).

It is interesting to note that the gel point of 0.05 or less implied by Fig. 2 compares well with that estimated from gravity batch settling in short tubes, this being 0.05 as well. It also highlights that both measurement and prediction of the shear and compressive yield stress of aggregated suspensions can be complimentary. Knowing that there is a simple method to predict the relationship between the shear and compressive yield stress and that both are scalar, measurement of full data sets as a function of solids concentration is now not a necessary condition to fully characterise

a particulate suspension in shear and compression. Indeed, many laboratories are limited in the range of stresses that can be measured accurately using a vane tool on a simple rheometer and equally, measurement of the full compressibility curve for some materials, especially biological materials that show non-quadratic filtration behaviour and those with a very low gel point [45] require a range of techniques (sedimentation, centrifugation and filtration) to measure data across a wide range of volume fractions [46]. The analysis of the data is equally complicated [47]. Equally, it is easier for many systems to measure data close to the gel point through compression using sedimentation, at intermediate solids through shear, and at very high solids in compression using filtration. There now exists the possibility to exploit the measurement techniques over a particular solids range in both shear and compression that are easiest for a particular sample to produce a comprehensive characterisation in both shear and compression.

4 Conclusions

The scaling of compressive strength data for nominally spherical particles shown here strongly favours the simple ‘ratchet elastic’ constitutive model encoded in Eqs. 3 and 4. The fact that both particle size [27] and now, apparently, shape can be scaled together in Fig. 1a is remarkable. That the compressive strength can be predicted from shear data provides further support for the model embodied in Eqs. 3 and 4. That this simple model cannot account for irreversibility without hand waving, nor for critical or yield-like behaviour, is of concern although wall adhesion may suffice

to alleviate these concerns. It certainly looks as if it can in principle, but whether it does or not quantitatively is another matter, although work aimed at finding out is in progress. Inaccuracies in the data are only likely at concentrations close to the gel point and in measurements where the wall adhesion is expected to be a significant contributor to the total measured stress. Truncation of the analysis and appropriate choice of measurement apparatus can reduce the errors significantly. Overall, the data analysis and fitting presented herein indicate a new future for the characterisation of aggregated particulate suspensions in shear and compression whereby a limited data set in both compression and shear, albeit targeted across a wide concentration range, can now be used to predict comprehensive curves for the shear yield stress and compressive yield stress of samples using a simple poro-elastic model. The veracity of the approach is indicated through a knowledge that the behaviour of both parameters is scalar across a wide range of materials and across a wide range of states of aggregation.

Acknowledgements The authors acknowledge the seminal work of PC Kapur in collecting and scaling a large amount of the original shear yield stress data from our laboratories and congratulate him on a wonderful career in science and engineering. The authors acknowledge the funding support from the Australian Research Council for the ARC Centre of Excellence for Enabling Eco-Efficient Beneficiation of Minerals, grant number CE200100009.

Funding Open Access funding enabled and organized by CAUL and its Member Institutions.

Declarations

Conflict of interest The authors confirm that neither them, their relatives or any business with which they are associated have any personal or business interest in or potential for personal gain from any of the organisations or projects linked to this manuscript.

Open Access This article is licensed under a Creative Commons Attribution 4.0 International License, which permits use, sharing, adaptation, distribution and reproduction in any medium or format, as long as you give appropriate credit to the original author(s) and the source, provide a link to the Creative Commons licence, and indicate if changes were made. The images or other third party material in this article are included in the article's Creative Commons licence, unless indicated otherwise in a credit line to the material. If material is not included in the article's Creative Commons licence and your intended use is not permitted by statutory regulation or exceeds the permitted use, you will need to obtain permission directly from the copyright holder. To view a copy of this licence, visit <http://creativecommons.org/licenses/by/4.0/>.

References

- Johnson S B, Franks G V, Scales P J, Boger D V, and Healy T W, *International Journal of Mineral Processing* **58** (1–4), (2000) 267.
- Nguyen Q D, and Boger D V, *Journal of Rheology* **27** (1983) 321.
- Nguyen Q D, and Boger D V, *Journal of Rheology* **29** (1985) 335.
- Leong Y K, Boger D V, Scales P J, and Healy T W, and R. Buscall, *Journal of the Chemical Society-Chemical Communications* **7** (1993) 639.
- Leong Y K, Scales P J, Healy T W, Boger D V, and Buscall R, *Journal of the Chemical Society-Faraday Transactions* **89** (14), (1993) 2473.
- Biggs S, Scales P J, Leong Y K, and Healy T W, *Journal of the Chemical Society-Faraday Transactions* **91** (17), (1995) 2921.
- Leong Y K, Scales P J, Healy T W, and Boger D V, *Journal of the American Ceramic Society* **78** (8), (1995) 2209.
- Colic M, Fisher M L, and Franks G V, *Langmuir* **14** (21), (1998) 6107.
- Franks G V, Johnson S B, Scales P J, Boger D V, and Healy T W, *Langmuir* **15** (13), (1999) 4411.
- Kapur P C, Scales P J, Boger D V, and Healy T W, *AICHE Journal* **43** (5), (1997) 1171.
- Scales P J, Johnson S B, Healy T W, and Kapur P C, *AICHE Journal* **44** (3), (1998) 538.
- Barnes H A, and Walters K, *Rheologica Acta* **24** (4), (1985) 323.
- Pashias N, Boger D V, Summers J, and Glenister D J, *Journal of Rheology* **40** (1996) 1179.
- Pham K, Petekidis G, Vlassopoulos D, Egelhaaf S, Poon W, and Pusey P, *Journal of Rheology* **52** (2), (2008) 649.
- Koumakis N, and Petekidis G, *Soft Matter* **7** (2011) 2456.
- Buscall R, Scales P J, Stickland A D, Teo H-E, and Lester D R, *JNNFM* **221** (2015) 40.
- Kusuma T E, Scales P J, Buscall R, Lester D, and Stickland A D, *Journal of Rheology* **65** (2021) 355.
- Channell G M, and Zukoski C F, *AICHEJ* **43** (1997) 1700.
- Green M D, Eberl M, and Landman K L, *AICHE Journal* **42** (1996) 2308.
- Zhou Z, Solomon M J, Scales P J, and Boger D V, *Journal of Rheology* **43** (1999) 651.
- Zhou Z W, Scales P J, and Boger D V, *Chemical Engineering Science* **56** (9), (2001) 2901.
- Usher S P, Scales P J, and White L R, *AICHE Journal* **52** (2006) 986.
- Lester D R, Usher S P, and Scales P J, *AICHE Journal* **51** (4), (2005) 1158.
- Usher S P, Studer L J, Wall R C, and Scales P J, *Chemical Engineering Science* **93** (2013) 277.
- Buscall R, *Colloids and Surfaces* **5** (1982) 269.
- Kapur P C, Raha S, Usher S P, de Kretser R G, and Scales P J, *Journal of Colloid and Interface Science* **256** (1), (2002) 216.
- de Kretser R G, Scales P J, and Boger D V. in *Rheology Reviews 2003*, (eds) Binding D M, and Walters K, British Society of Rheology, Aberystwyth (2003), pp 125–166.
- Kim C, Liu Y, Kuehnle A, Hess S, Viereck S, Danner T, Mahadevan L, and Weitz D A, *Physical Review Letters* **99** (2007) 028303.
- Lietor-Santos J J, Kim C, Lu P J, Fernandez-Nieves A, and Weitz D A, *The European Physical Journal E* **28** (2), (2009) 159.
- Michaels A S, and Bolger J C, *I&EC Fundamentals* **1** (1), (1962) 24.
- Lester D R, Buscall R, Stickland A D, and Scales P J, *Journal of Rheology* **58** (5), (2014) 1247.
- Lester D, and Buscall R, *Journal of Non-Newtonian Fluid Mechanics* **221** (2015) 18.
- Buscall R, *Colloids and Surfaces* **43** (1), (1990) 33.
- Aziz A A A, Dixon D R, Usher S P, and Scales P J, *Colloids and Surfaces A* **290** (1–3), (2006) 194.

35. Holland, F.A. and F.S. Chapman, *Liquid mixing and processing in stirred tanks*. 1966, New York: Reinhold Publishing Corporation. 319.
36. de Kretser R G, Usher S P, Scales P J, Boger D V, and Landman K A, *AIChE Journal* **47** (8), (2001) 1758.
37. Usher S P, de Kretser R G, and Scales P J, *AIChE Journal* **47** (7), (2001) 1561.
38. Buscall R, and Lester D R, *AIChE Journal* **63** (5), (2017) 1520.
39. Green M D, and Boger D V, *Industrial and Engineering Chemical Research* **36** (11), (1997) 4984.
40. de Kretser R G, Stickland A D, Usher S P, and Scales P J. in *FILTECH*, Wiesbaden, Germany (2011), pp I383–I340.
41. Seto R, Auernhammer G K, Botet R, Meireles M, and Cabane B, *Journal of Rheology* **57** (5), (2013) 1347.
42. Mills P, Goodwin J, and Grover B, *Colloid and Polymer Sci.* **269** (1991) 949.
43. Stickland A D, Kumar A, Kusuma T E, Scales P J, Tindley A, Biggs S R, and Buscall R, *Rheol. Acta* **54** (5), (2015) 332.
44. Firth B A, *Journal of Colloid and Interface Science* **57** (1976) 257.
45. Stickland A D, De Kretser R G, and Scales P J, *AIChE Journal* **51** (9), (2005) 2481.
46. Skinner S J, Studer L J, Dixon D R, Hillis P, Rees C A, Wall R C, Cavalida R G, Usher S P, Stickland A D, and Scales P J, *Water Research* **82** (2015) 2.
47. Skinner, S.J., A.D. Stickland, and P.J. Scales, *Dewatering characterisation and modelling: An extremely compressible approach*, in *Filtrieren and Separieren Global Guide of the Filtration and Separation Industry 2018–2020*. 2018. p. pp. 211– 221.

Publisher's Note Springer Nature remains neutral with regard to jurisdictional claims in published maps and institutional affiliations.